THE STUDY OF THE SPACE CHARGE EFFECTS FOR RCS/CSNS

S. –Y. Xu, S. –X. Fang, S. Wang#
Institute of High Energy Physics (IHEP), Beijing, 100049, China

Abstract

RCS is a key component of CSNS. In this kind of high intensity RCS, the beam is space charge dominated, and the space charge effects are the main source of beam loss. Many simulation works were done for the study of space charge effects for CSNS/RCS by using code ORBIT and SIMPSONS.

INTRODUCTION

The China Spallation Neutron Source (CSNS) is an accelerator-based facility. It operates at 25 Hz repetition rate with an initial design beam power of 100 KW, and is capable of upgrading to 500KW. CSNS consists of a 1.6 GeV Rapid Cycling Synchrotron (RCS) and a 80 MeV linac, which can be upgraded to 250-MeV for beam power upgrading to 500 KW. RCS accumulates 80 MeV injection beam, and accelerates the beam to the design energy of 1.6 GeV, and extracts the high energy beam to the target. The lattice of the CSNS/RCS is a triplet based four-fold structure. Table 1 shows the main parameters of the lattice [1].

Due to the high beam density and high repetition rate, the rate of beam loss must be controlled to a very low level. In this kind of high power RCS, especially in the low energy end, the beam is space charge dominated, and the space charge effects can result in emittance growth and halo formation, which may contribute to beam losses. The space Charge effects are the most important issue of CSNS/RCS, which limit the maximum beam intensity, as well as the beam power. Many simulations works were done to study the space charge effects of CSNS/RCS by using the codes ORBIT and SIMPSONS. The simulation results are the foundation of physics design and the choice of design parameters.

SPACE CHARGE EFFECTS DURING INJECTION

In order to decrease the longitudinal beam loss, the longitudinal injection scenario with 50% chopping rate is adopted. In the CSNS, anti-correlated painting is employed to obtain a large transverse beam size which can significantly reduce the space charge tune shift of the accumulated beam. The emittance is painted from small to large in horizontal direction, while from large to small in vertical direction during 200-turn injection in 0.39 ms, with peak linac beam current of 15 mA.

During injection, the kinetic linac beam is fixed, while the kinetic energy of the synchronous particle in the CSNS/RCS varies with the dipole field B of the RCS:

$$E_K = E_0(\sqrt{1+6.569\mathrm{B}^2(T)}-1) \quad (1)$$

where E_0 is the rest energy of proton.

Table 1: Main Parameters of the Lattice

Circumference (m)	227.92
Superperiod	4
Number of dipoles	24
Number of long drift	12
Total Length of long drift (m)	75
Betatron tunes (h/v)	4.86/4.78
Chromaticity (h/v)	-4.3/-8.2
Momentum compaction	0.041
RF harmonics	2
RF Freq. (MHz)	1.0241~2.444
RF Voltage (kV)	165
Trans. acceptance (μπm.rad)	540

To obtain a uniform longitudinal distribution, to reduce the transverse space charge effects, the starts of injection should be carefully chosen. By comparing the longitudinal distribution with different start time, -0.14 ms was chosen, and the beam is injected from -0.14 ms to 0.25 ms. The deviations of the kinetic energy of the injected particle from that of the synchronous particles in the RCS during injection are shown in Fig. 1 (a). Figure 1 (b) shows the beam distribution in the longitudinal phase space at the end of injection.

In case of no space charge effects, to obtain a uniform distribution in horizontal and vertical phase space, the bump functions are given by:

$$x(t) = x_0\sqrt{\frac{t}{t_{inj}}}, \quad 0 \le t \le t_{inj} \quad (2)$$

$$y(t) = y_0\sqrt{\frac{t_{inj}-t}{t_{inj}}}, \quad 0 \le t \le t_{inj} \quad (3)$$

where t_{inj} is the injection time, and x_0, y_0 are the radiuses of the normalized horizontal and vertical phase space.

wangs@ihep.ac.cn

Figure 2 shows the painted beam distribution in vertical direction by using bump functions of Eq. (2) and Eq. (3), in which (a) is the painting without space charge effects, and (b) shows the painted distribution with space charge effects. It can be observed that with space charge effects, the beam distribution deviates from the uniform distribution obviously, and some halo particles are generated.

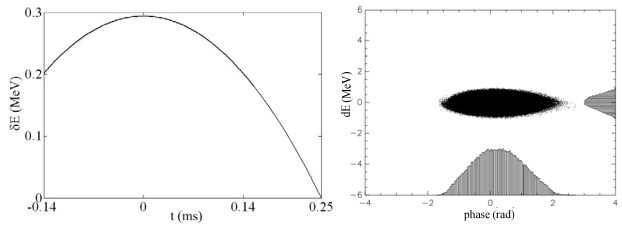

Figure 1: (a): The deviations of the energy of the injected particle from that of the synchronous particle in the RCS during injection; (b): The beam distribution in longitudinal phase space at the end of injection.

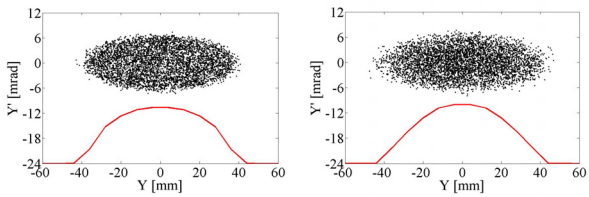

(a) (b)

Figure 2: Beam distributions in vertical phase space at the end of injection with (b) and without (a) space charge effects.

For anti-correlated painting, the beam distribution in the real space is not uniform during the injection as shown in Fig. 3 (a), which shows the distribution after 20 turns injection without space charge effects. The Lorentz force experienced by particles is shown in Fig. 3 (b). The Lorentz force drives the particles move towards the inner and outer region in the vertical phase space, and the beam distribution is changed from the uniform distribution.

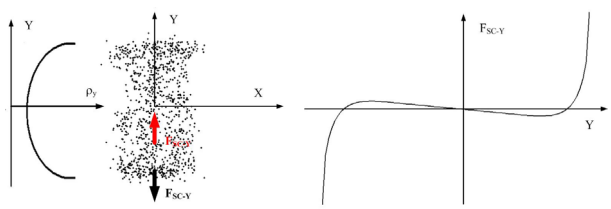

(a) (b)

Figure 3: The distribution in the real space after 20 turns injection without space charge effects, and the Lorentz force experienced by particles considering space charge effects.

In order to produce a much uniform transverse distribution and reduce halo production, the bump function is optimized by injecting less particles in the inner and outer region of the emittance space. Then the bump functions are given as:

$$y = \sqrt{\frac{y_0^2}{2} + \frac{y_{\max}^2 - \frac{y_0^2}{2}}{(\frac{t_{inj}}{2})^{3/2}}(\frac{t_{inj}}{2} - t)^{3/2}} \quad for \quad 0 < t < \frac{t_{inj}}{2} \tag{4}$$

$$y = \sqrt{\frac{y_0^2}{2} - \frac{\frac{y_0^2}{2} - y_{\min}^2}{(\frac{t_{inj}}{2})^{3/2}}(t - \frac{t_{inj}}{2})^{3/2}} \quad for \quad \frac{t_{inj}}{2} < t < t_{inj} \tag{5}$$

where $y_{max}<y_0$, $y_{min}>0$ are the maximum and minimum bumps during injection. Figure 4 shows 1-D density profiles in vertical direction for different bump functions. The distribution in the vertical phase space painted with new bump functions is more uniform than the distribution painted with bump described by Eq. (2), and (3).

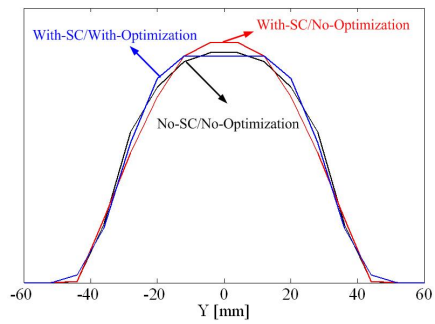

Figure 4: 1-D density profile in vertical direction. X-axis: beam size in mm; Y-axis: density in arbitrary units.

SPACE CHARGE EFFECTS DURING ACCELERATION

To study the space charge effects during the acceleration in a cycle, two initial transverse beam distributions are employed, one is the KV distribution, and the other is the real distribution obtained by anti-correlated painting by using optimized bump functions.

For the initial KV distribution with the unnormalized rms emittances of 60 πmm·mrad in both horizontal and vertical directions, Figure 5 shows the time evolution of unnormalized rms emittances. There is strong transverse coupling induced by space charge. Space charge may lead to emittance exchange through space charge coupling in high current synchrotrons. The space charge coupling is an internal resonance driven by the self-consistent space charge potential of coherent eigenmodes [5][6]. Figure 6 (b) shows the forth order model, which has the space charge potential of x^2y^2, already developed by 200 turns [9]. The working point (4.86, 4.78) is close to the resonance $2\upsilon_x-2\upsilon_y=0$, which is driven by the fourth order coupling term x^2y^2 in the Hamiltonian. The emittance

exchange is probably caused by the resonance $2\upsilon_x$-$2\upsilon_y$=0.

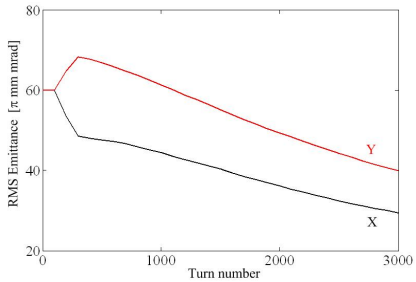

Figure 5: The time evolution of unnormalized rms emittances at the early stage.

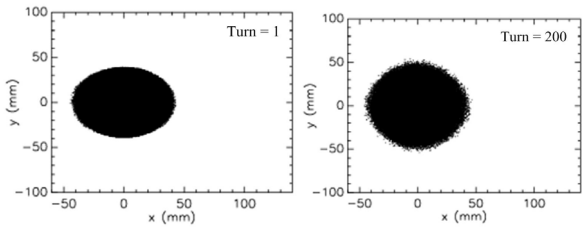

(a) (b)

Figure: 6 Beam distributions in (x, y) real space. (a): Distribution at the first turn; (b): Distribution at the 200th turn.

The resonance $2\upsilon_x$-$2\upsilon_y$=0 was first analyzed by Montague [8]. This resonance can occur even for a linear lattice without any perturbations since it requires only a zero harmonic in the Fourier component of the density perturbation. Due to the fact that this resonance is a difference resonance, such coupling can lead to a significant effect for a beam with unequal emittances [8][10]. The unperturbed KV system has no coupling. Some small density fluctuation in the numerically generated initial KV distribution and different beam parameters resulting from the rms matching procedure may lead to exponential growth of the eigenmode with the potential of x^2y^2, which is capable of exciting the Montague resonance [5][7].

Figure7 shows the simulation results with initial real distribution. Different from the results of using initial KV distribution, there is no great rms emittance exchange, and no high-order collective beam mode is observed. A possible explanation might be that in the real beam a finite spread of single particle frequencies leads to Landau damping and suppression of instabilities for some modes [5][6][7].

In the simulations with initial real distribution, diffusion of particles among different parts in the phase space occurs during acceleration. In order to study the mechanisms, 30 test particles were set in the simulations by SIMPSONS. The test particles were chosen so as to cover the entire region of interest. The poincaré maps of most of test particles are distorted during acceleration. For test-particle-A, the time evolution of the C-S invariant is shown in Fig. 8, and space charge coupling resonance seems to be excited.

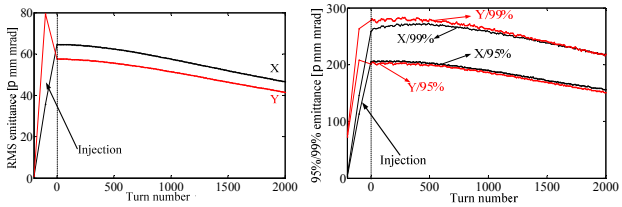

(a) (b)

Figure 7: The time evolution of the unnormalized emittances at the early stage. (a): rms emittance; (b): 99% emittance.

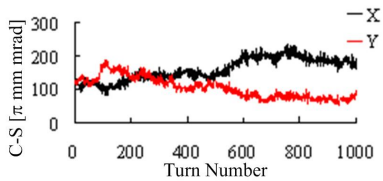

Figure 8: The time evolution of the C-S invariant of test-particle-A.

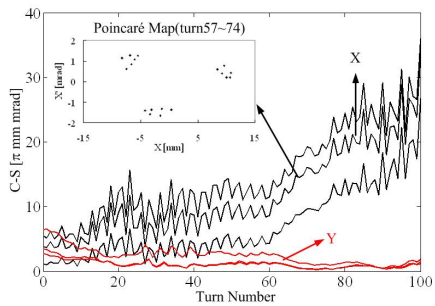

Figure 9: The time evolution of the C-S invariant of test-particle-C/D/E.

Figure 9 shows the time evolution of the C-S invariant of test-particle-C/D/E. The resonance $3\upsilon_x$=14 is probably excited. The dynamics feature of test-particle-F is complicated, and the time evolution of the C-S invariant is shown in Fig. 10. Figure 11 shows poincaré maps in horizontal direction during 625-649 turns and in vertical direction during 637-652 turns. The horizontal C-S invariant growth of test-particle-F during 57-74 turns is probably caused by the resonance $3\upsilon_x$=14, and during 625-649 turns by $5\upsilon_x$=23. During 637-652 turns the resonance $2\upsilon y$=9 is probably excited which results in the vertical C-S invariant growth.

The simulation results show that, a resonance becomes dominant during one time-period, and another resonance may be driven during another time-period. The chaos motion appears in this procedure, and some particles move to the outside of the beam core and become halo particles.

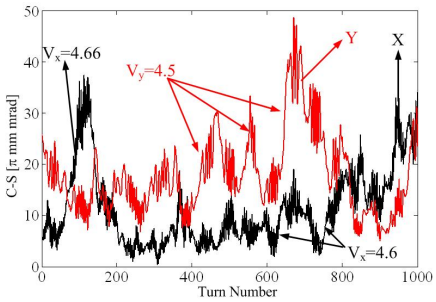

Figure 10: The time evolution of the C-S invariant of test-particle-F.

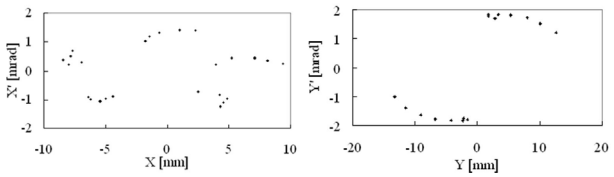

Figure 11 (a): The poincaré map in horizontal direction during 625-649 turns; (b): The poincaré map in vertical direction during 637-652 turns.

SPACE CHARGE EFFECTS VS. TUNES

In the simulations to study the dependence of emittance growth on tunes, also two kinds of initial transverse distribution: KV distributions and the real distributions obtained by anti-correlated painting are adopted. Tunes around design values of 4.86/4.78 were compared. In simulations with initial KV distribution, the normalized rms emittance of 25πmm·mrad in both horizontal and vertical directions is used. The strong coupling was observed, and is dependent on the tunes. Figure 12 shows the normalized rms emittance exchange depending on tunes. For the KV distribution, the emittance exchange for υ_x-υ_y>0.12 and υ_x=υ_y is absent. For the case υ_x-υ_y>0.12, the Montague resonance is avoided by sufficient splitting of the tunes. The working point of CSNS/RCS can be adjusted to (5.82, 4.80), for which the Montague resonance can be avoided. Due to the fact that the Montague resonance is a difference resonance, such coupling can lead to a significant effect for a nonequipartitioned beam. In addition "free energy" is required for driving the instability, which stems from the energy anisotropy between different degrees of freedom [7][10]. For the case of υ_x=υ_y, there is no emittance exchange, because the beam is equipartitioned, and the "free energy" is absent for driving the instability.

As discussed in the section of "space charge effects during acceleration", no high-order collective beam mode and great rms emittance exchange are observed in the simulations with initial real distribution generated by the anti-correlated painting. It is completely different from the results of initial KV distribution. But for the tunes close to m(υ_x-υ_y)=0, there is large 99% emittance growth in vertical direction, as shown in Fig. 13. For these tunes, the resonance m(υ_x-υ_y)=0 may be excited for much particles, and then results in the vertical C-S invariant growth. As a result, the 99% emittance grows.

SUMMARY

Space charge effects have been studied by simulations, including the space charge effects in painting, accelerating, and the dependence of space charge effects on the bare tune. Some injection painting optimizations were made to obtain a much uniform distribution.

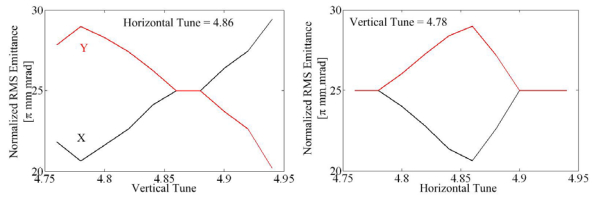

(a) (b)

Figure 12: The dependence of coupling on tunes. (a): For fixed υ_x=4.86; (b): For fixed υ_y=4.78.

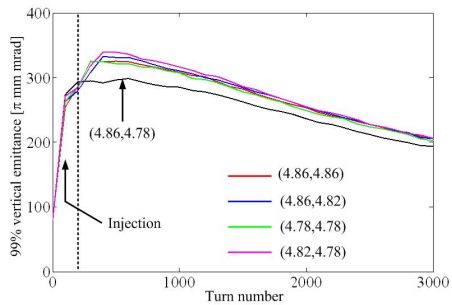

Figure 13: The time evolution of unnormalized 99% emittances at the early stage of acceleration with different tunes.

ACKNOWLEDGMENT

The authors would like to thank Dr. Shinji Machida for providing us the SIMPSONS code and with help on test run.

REFERENCES

[1] CSNS Feasibility Study Report, June, 2009, IHEP.
[2] Shinji Machida, "The Simpsons Program User's Reference Manual", July, 1992.
[3] J. Galambos, J. Holmes, D. Olsen, ORBIT "Use's Manual, V.1.0", SNSORNL-AP, Tech. Note 11, March 1999.
[4] J. Beebe-Wang, A. V. Fedotov and J. Wei, Proceedings of the EPAC 2000,Vienna, Austria, 26-30 June 2000, p.1286-1288.
[5] A.V. Fedotov, J. Holmes and R.L. Gluckstern, "Instabilities of high-order beam modes driven by space-charge coupling resonances", Phys. Rev. ST AB 4,084202 (2001).
[6] I. Hofmann and O. Boine-Frankenheim, "Resonant Emittance Transfer Driven by Space Charge", Phys. Rev. L. 87, 034802 (2001).
[7] I. Hofmann, J. Qiang, R. D. Ryne, "Collective Resonance Model of Energy Exchange in 3D Nonequipartitioned Beams" Phys. Rev. Lett. 86, 2313, (2001).
[8] B.W. Montague, CERN Report 68-38 (1968).

[9] I. Hofmann, Phys. Rev. E 57, p. 4713 (1998).
[10] A. V. Fedotov et al, "Excitation of resonances due to the space charge and magnet errors in the SNS ring", PAC'01, p. 2848 (2001).